

Supplementary material for:

Perceptual re-learning of complex visual motion after V1 damage in humans

Krystel R. Huxlin, Tim Martin, Kristin Kelly, Meghan Riley, Deborah I. Friedman, W. Scott
Burgin and Mary Hayhoe

This file includes:

Supplementary Table 1

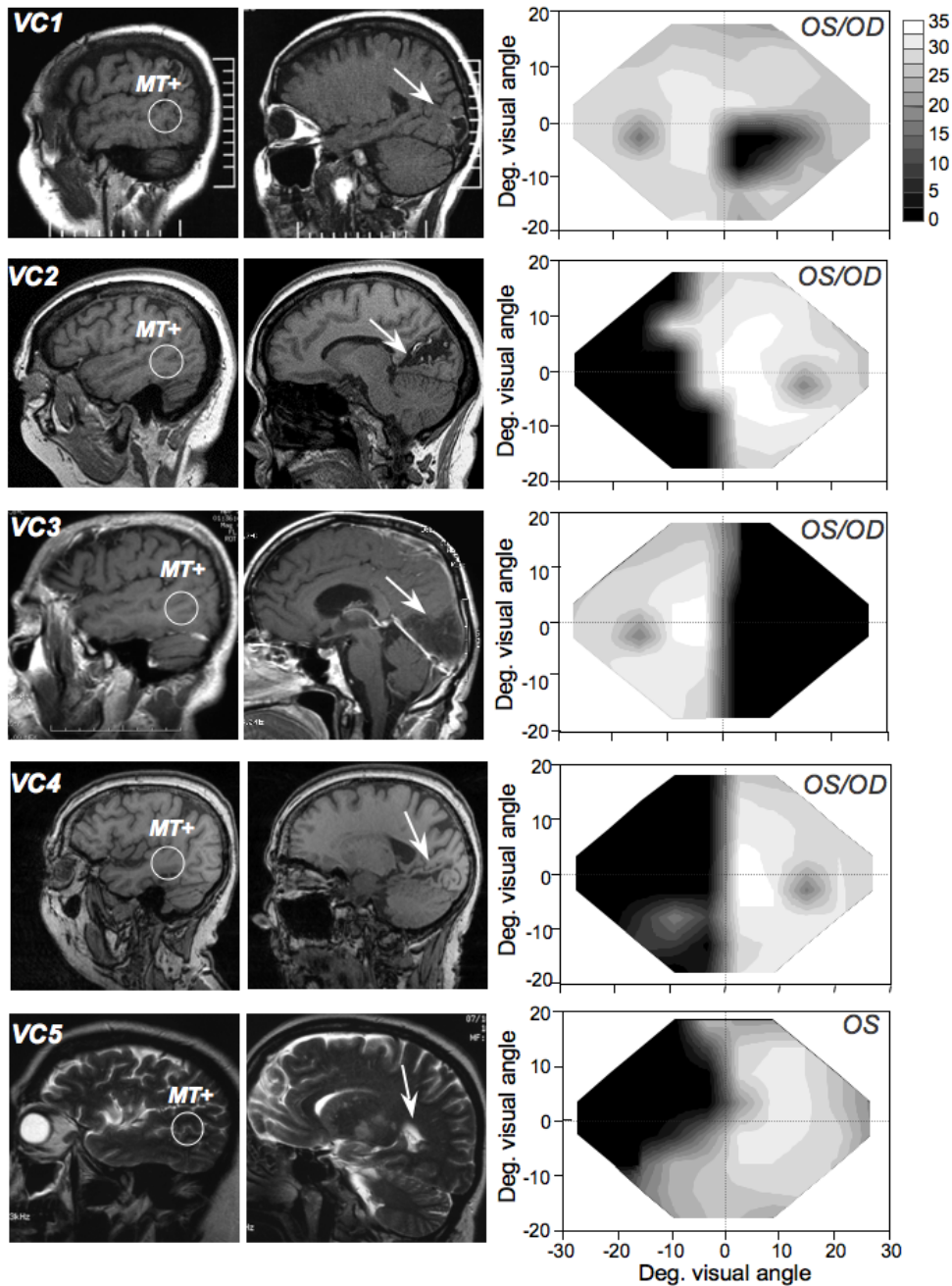
Supplementary Figs. S1-5

Supplementary Table 1. Participant demographics

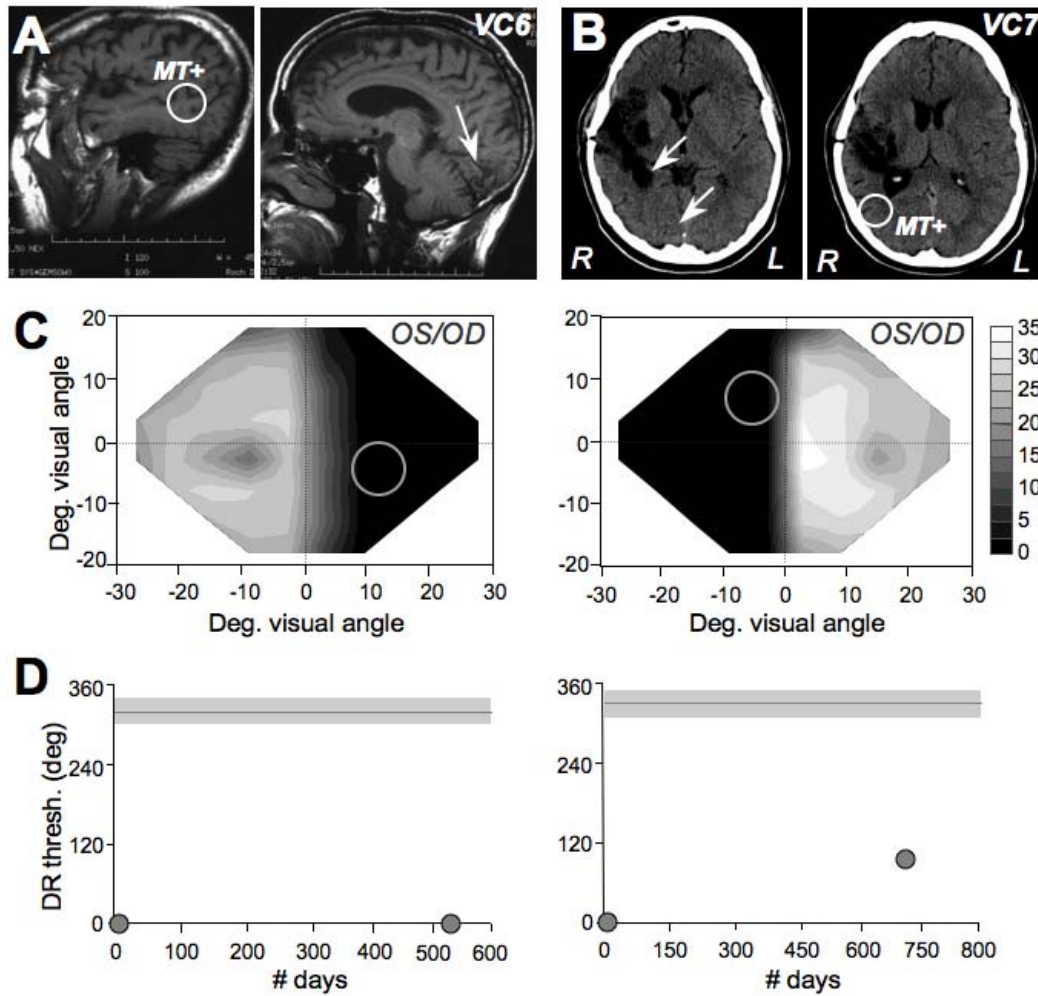
	VC1	VC2	VC3	VC4	VC5	VC6	VC7
Gender	Female	Female	Male	Female	Female	Male	Male
Age (years)	51	65	51	68	50	83	32
Handedness	Right	Right	Right	Right	Right	Right	Right
OR/V1 damage	Yes	Yes	Yes	Yes	Yes	Yes	Yes
Time since lesion (mths)	14	8	20	14	40	12-29*	12
Affected hemifield	Right	Left	Right	Left	Left	Right	Left
Visual acuity OS	20/15	20/20	20/15	20/20	20/40	20/200 _c	20/20
Visual acuity OD	20/25	20/20	20/15	20/20	20/400 _p	20/100 _c	20/20
Corrective lenses	Yes	Yes	Yes	Yes	Yes	Yes	No
Mobility aids	No	No	No	No	No	No	No
Able to drive	Yes	Yes	Yes	Limited	Yes	No	Yes

OR - optic radiation; V1 – primary visual cortex; OS – left eye; OD – right eye
p - long-standing effect due to prior episode of central vasculitis in the right eye.
c - secondary to cataract removal bilaterally

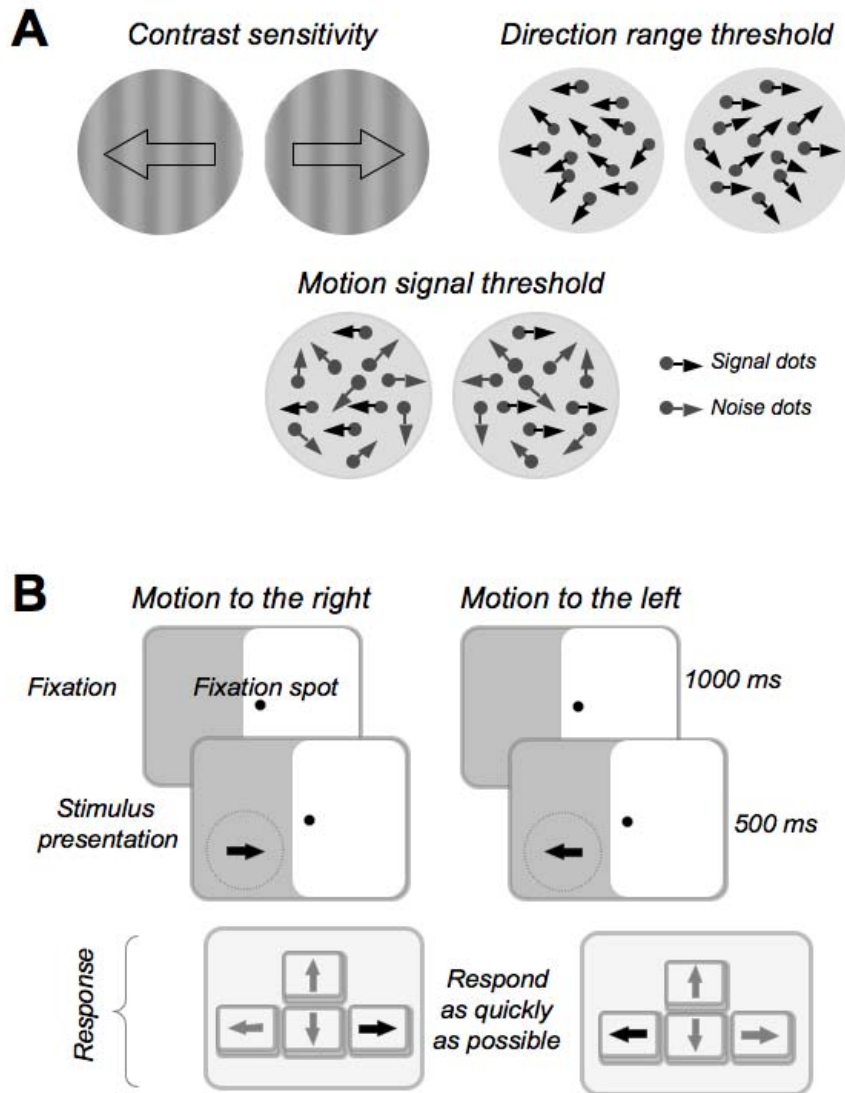
* - VC6 had 3 strokes, each damaging the occipital lobes. The first occurred 29 months before recruitment and the last, 12 months before recruitment.



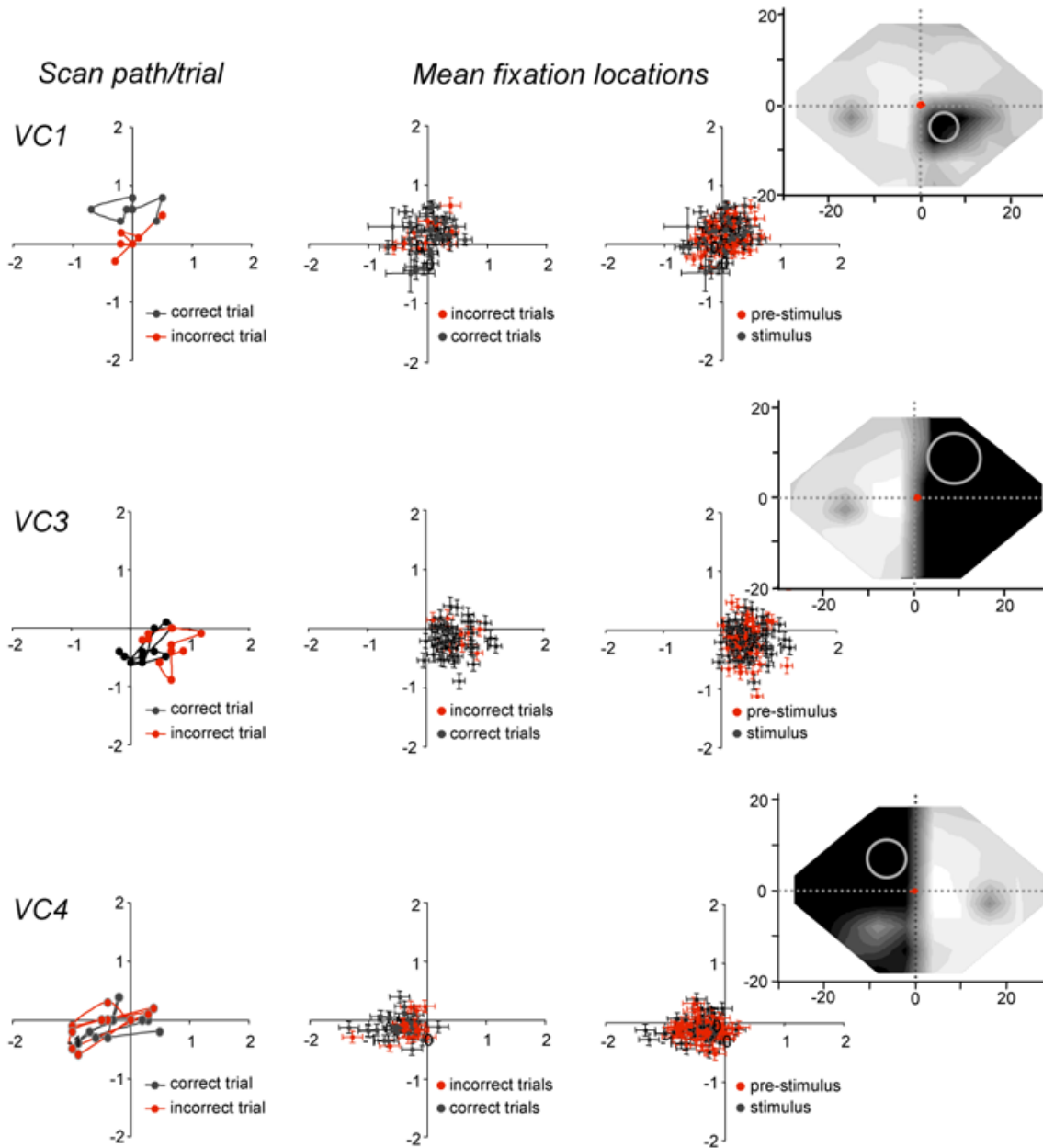
Supplementary Figure 1. Structural MRI and Humphrey perimetry for VC1-5. Post-stroke magnetic resonance images in the parasagittal plane, collected about 40-50mm lateral to the midline and 10mm lateral to the midline respectively. The MT+ complex (white circles) appear intact in the most lateral images. The region of tissue damage in the occipital lobe is indicated by a white arrow in the more medial images. Iso-sensitivity maps are shown for each subject, illustrating the extent of their visual field defect. They were created by averaging dB values at each sampling point in each subject's monocular 24-2 Humphrey fields (OS = left eye; OD= right eye). The only exception was VC5, whose right eye data was unusable because of macular [retinal] damage and the inability to fixate. Grey scale = visual sensitivity in dB. The blind spot (decrease in sensitivity due to the optic disc) is indicated in VC1-4's composite visual field maps.



Supplementary Figure 2. Structural MRI, Humphrey perimetry and direction range thresholds for untrained subjects VC6 and VC7. **A.** Lateral (40-50mm from midline) and medial (~10mm from midline) T1-weighted MRI images in the parasagittal plane collected after VC6's last stroke. Note the intact appearance of the MT+ complex (white circle) and the region of tissue damage in the left occipital lobe (white arrow). **B.** Horizontal CT scans collected after stroke in VC7. The damage appears to spare the MT+ complex (white circle), affecting primarily the right temporal lobe and the optic radiations leading up to V1 (white arrows). **C.** Iso-sensitivity maps are shown for each subject, illustrating the extent of their visual field defect (black regions). The maps were created by averaging dB values at each sampling point in each subject's monocular 24-2 Humphrey fields (OS = left eye; OD= right eye). Grey scale = visual sensitivity in dB. **D.** Plots of direction range threshold (red points) versus time elapsed (in days) in VC6 and VC7. Thresholds were measured under controlled fixation conditions in the laboratory, in the circular regions of the blind field indicated in C for both subjects. Data were collected more than 500 days apart, in order to assess whether spontaneous improvements in global motion processing could occur in the blind field following V1 damage. Spontaneous improvements were defined as improvements in direction range thresholds that occurred in the absence of any psychophysical training in the blind field. The mean (grey line) and standard deviation of the mean (grey shaded area around the grey line) direction range thresholds obtained at "control" locations in the intact hemifield of each subject are indicated on each graph for reference.



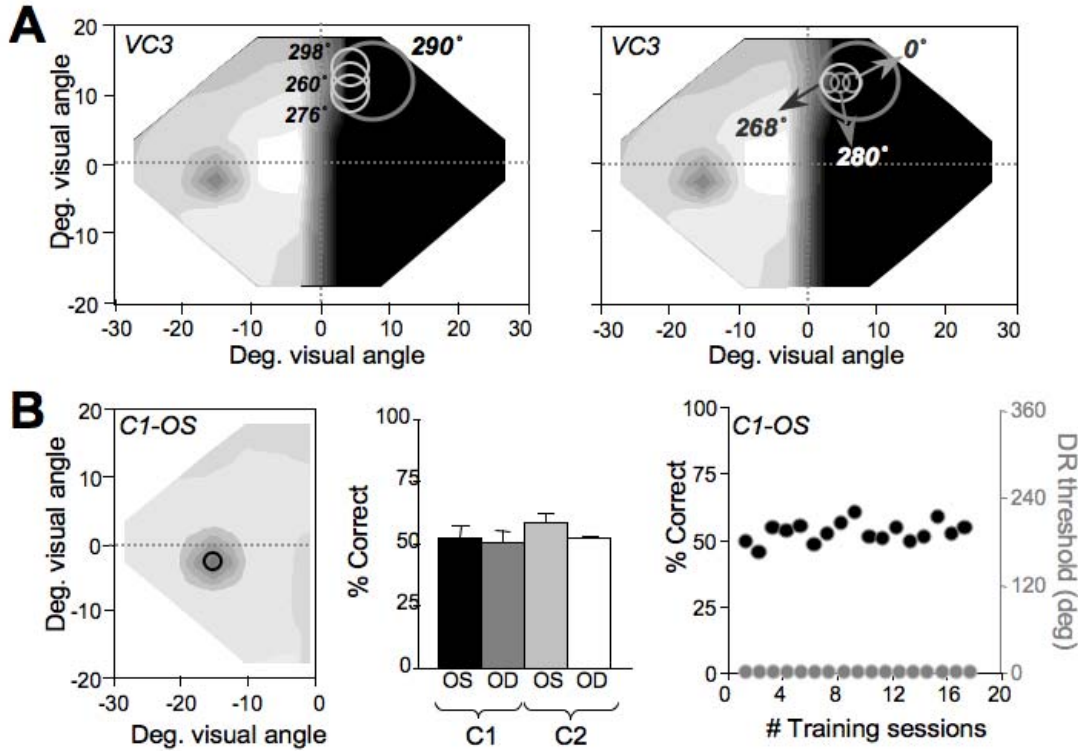
Supplementary Figure 3. Psychophysical training and testing methods. **A.** Stimuli used to measure simple and complex motion thresholds. Luminance-modulated, vertical sinewave gratings drifting to either the left or right, were used to measure simple motion perception (contrast sensitivity for direction). Grey dots randomly distributed within a circular aperture over a bright background and drifting in a range of direction centered around the left- or rightward vector were used to measure global direction discrimination. Grey dots randomly distributed within a circular aperture over a bright background and drifting either to the left- or right (signal dots) or randomly (noise dots) were used to measure motion signal thresholds. **B.** During both training and testing, subjects were required to perform a direction discrimination task that began by precisely fixating a target for 1000ms. A stimulus was then presented at a selected location in either the blind (grey area) or seeing portion of their visual field. After 500ms, both the stimulus and fixation spot disappeared, and subjects were asked to indicate the global direction of motion in the stimulus by pressing the right or left arrow keys on the computer keyboard as quickly as possible. This was immediately followed by auditory feedback that indicated the correctness of the response.



Supplementary Figure 4. Scan paths and mean eye position per trial during performance of the global direction discrimination task post-training in VC1, 3 and 4. Eye position data was collected using the ASL Mobile Eye tracker. Four plots are presented for each subject. The first graph provides examples of scan paths during stimulus presentation for two consecutive trials – one for which the subject responded correctly (black symbols – correct trial) and one for which the subject responded incorrectly (red symbols – incorrect trial). Eye positions (dots) are plotted at 50ms intervals during the 500ms stimulus presentation. The second graph for each subject plots the mean eye position relative to the fixation spot (0,0) during stimulus presentation, separated into correct and incorrect trials. Note that there are significantly fewer incorrect than correct trials since this is a retrained, blind field location where the subjects attained a normal direction range threshold. The complete overlap in eye positions between correct and incorrect trials suggests that subjects are not consistently moving their eyes towards the stimulus in order to perform correctly on this global direction discrimination task. This is further confirmed by the comparison, in the third graph, between eye positions in the 330ms preceding each stimulus onset (red symbols) and mean eye positions during stimulus presentation

Huxlin et al. Supplementary Material

(black symbols, correct and incorrect trials included). Again, there is complete overlap between eye positions during fixation, whether or not a stimulus is being presented in the blind field. The fourth graph is a composite Humphrey visual field map illustrating the extent of the visual deficit (black shading) for each subject, the location of the visual stimulus in the blind field during performance of the global direction discrimination task with Mobile Eye tracking, and the mean eye positions recorded with the tracker for each of the 50 trials performed during the testing session (red symbols). Note the tight clustering of the eye positions around the origin (fixation spot location) and the relatively distant position of the stimulus. All axes provide values in degrees of visual angle relative to the fixation spot (0,0). Error bars represent SEMs.



Supplementary Figure 5. Control experiments. A. Experiment to estimate the proportion of training stimulus actually utilized by subjects during blind field training. After global direction discrimination training in his blind field using a large, random dot stimulus, VC3 attained a direction range threshold of 290° at the retrained location. This performance level was maintained when the stimulus size was decreased to 5° in diameter (all other stimulus parameters remaining the same), and was positioned at the edge of the larger stimulus closest to the vertical meridian. By decreasing the probing stimulus size to 2° in diameter (all other parameters remaining the same), it was possible to show that perceiving a strip of the training stimulus about 4° wide was sufficient for VC3 to perform this task. **B.** Experiment to assess whether light scatter could be used to learn to extract global directional information from random dot stimuli placed within the blind spot of visually-intact control subjects C1 and C2. The visual field map on the left illustrates the position and size (2° in diameter) of the random dot stimulus used to measure direction range thresholds within the left blind spot of C1. The stimulus was identical to stimuli used to train VC1-5 except for its smaller size and brightness. The adjacent histogram plots percent correct performance on this task for four eyes (OS=left eye, OD=right eye) from C1 and C2. Performance was not significantly different than chance (50% correct on this task). The third graph plots % correct performance on the left axis (black symbols) and direction range (DR) thresholds on the right axis (grey symbols) for the left eye (OS) of subject C1, who underwent daily global direction discrimination training with a random dot stimulus placed in her blind spot for a period of 17 days. No improvement in % correct or direction range threshold performance was noted over this period of time.